

The Optical Gravitational Lensing Experiment.
***UBVI* Photometry of Stars**
in Baade's Window*

B. Paczyński¹, A. Udalski²,
M. Szymański², M. Kubiak²,
G. Pietrzyński², I. Soszyński²,
P. Woźniak¹, and K. Żebruń²

¹ Princeton University Observatory, Princeton, NJ 08544-1001, USA
 e-mail: (bp,wozniak)@astro.princeton.edu

²Warsaw University Observatory, Al. Ujazdowskie 4, 00-478 Warszawa,
 Poland

e-mail: (udalski,msz,mk,pietrzyn,soszynsk,zebrun)@sirius.astrouw.edu.pl

ABSTRACT

We present *UBVI* photometry for 8530 stars in Baade's Window obtained during the OGLE-II microlensing survey. Among these are over one thousand red clump giants. 640 of them have photometry with errors below 0.05 mag. We constructed a map of interstellar reddening. The corrected colors of the red clump giants: $(U-B)_0$, $(B-V)_0$, and $(V-I)_0$ are very well correlated, indicating that a single parameter determines the observed spread of their values, reaching almost 2 mag in the $(U-B)_0$. It seems most likely that heavy element content is the dominant parameter, but it is possible that another parameter: the age (or mass) of a star moves it along the same trajectory in the color-color diagram as the metallicity. The current ambiguity can be resolved with spectral analysis, and our catalog may be useful as a finding list of red clump giants. We point out that these K giants are more suitable for a fair determination of the distribution of metallicity than brighter M giants.

We also present a compilation of *UBVI* data for 309 red clump giants near the Sun, for which Hipparcos parallaxes are more accurate than 10%. Spectral analysis of their metallicity may provide information about the local metallicity distribution as well as the extent to which mass (age) of these stars affects their colors.

It is remarkable that in spite of a number of problems, stellar models agree with observations at the 0.1–0.2 mag level, making red clump giants not only the best calibrated but also the best understood standard candle.

*Based on observations obtained with the 1.3 m Warsaw telescope at the Las Campanas Observatory of the Carnegie Institution of Washington.

1 Introduction

Red clump giants appear to be one of the best standard candles available. Not a single RR Lyrae star or a Cepheid has its parallax measured by Hipparcos (Perryman *et al.* 1997) with a 10% accuracy (Horner *et al.* 1999), but there are about 10^3 red clump giants with parallaxes at least as good as 10% (Paczynski and Stanek 1998). The absolute I -band magnitude of these stars appears to be almost independent of their $(V - I)$ color (Paczynski and Stanek 1998). The weak dependence on metallicity was empirically calibrated by Udalski (1998a), who also demonstrated that there is no detectable dependence on age, as long as it is between 2×10^9 and 10×10^9 years (Udalski 1998b). While this calibration is not perfect, it is superior to the calibration of either RR Lyrae or Cepheid variables, or any other standard candle ever proposed. Unfortunately, there is some confusion about the color–metallicity dependence (Paczynski 1998).

The main purpose of this paper is to present a catalog of $UBVI$ photometry for 8530 stars in Baade’s Window obtained during the second phase of the Optical Gravitational Lensing Experiment (OGLE-II) microlensing project (*cf.* Udalski, Kubiak and Szymański 1997). The important part of the catalog is the list of 640 red clump giants in the galactic bulge/bar, covering a very broad range of colors, and presumably metallicities. We also present a compilation of $UBVI$ photometry (Mermilliod and Mermilliod 1994) for 309 nearby red clump giants, for which Hipparcos parallaxes are more accurate than 10%. Our expectation is that these two data sets provide a convenient list of objects for which metallicity can be obtained spectroscopically in order to determine the range of $[\text{Fe}/\text{H}]$ and $[\text{O}/\text{H}]$ for nearby stars as well as for those near the Galactic center. Such spectroscopic study could resolve the current ambiguity about the distribution of metallicities and the relation between the metallicity and colors of red clump giants.

We also present, following Kiraga, Paczynski and Stanek (1997), a description of the procedure which appears to be fairly accurate in mapping interstellar extinction. The variation, with the line of sight, of average colors of the bulge red clump stars, red sub-giants, and the stars near the main sequence turn off point are very well correlated with each other, as all are affected by the same variations in the interstellar reddening. The map of color variations provides information about angular scale over which the extinction varies.

2 Observations

Observations presented in this paper were collected during the second phase of the OGLE microlensing search with the 1.3-m Warsaw telescope at the Las Campanas Observatory, Chile which is operated by the Carnegie Institution of Washington. The telescope was equipped with the "first generation" camera with a SITe 2048×2048 CCD detector. The pixel size was $24 \mu\text{m}$ giving the 0.417 arcsec/pixel scale. Observations were performed in the "medium" speed reading mode of the CCD detector with the gain $7.1 \text{ e}^-/\text{ADU}$ and readout noise of about 6.3 e^- . Details of the instrumentation setup can be found in Udalski, Kubiak and Szymański (1997).

The *BVI* photometry comes from observations of the OGLE-II field covering large part of Baade's Window: BUL_SC45. Observations of this field were obtained in the drift-scan mode of the CCD detector and the field covers approximately 14.2×57 arcmin in the sky. Coordinates of its center are: $\text{RA}(\text{J2000}) = 18^{\text{h}}03^{\text{m}}36^{\text{s}}.5$, $\text{DEC}(\text{J2000}) = -30^{\circ}05'00''$. The effective exposure time was 87, 124 and 162 seconds for the *I*, *V* and *B*-band, respectively. BUL_SC45 field is observed in somewhat different way than the remaining 47 bulge fields – it is not a subject of microlensing search. Observations of this field are collected mainly for maintaining the phasing of variable stars discovered in its part during the first stage of the OGLE project (*cf.* Udalski *et al.* 1995). Therefore only about 30 *I*-band, 15 *V*-band and 10 *B*-band epochs were collected during the period August 5, 1997 through October 21, 1998.

The *U*-band photometry was obtained in the standard, still frame mode of the CCD detector. One field, covering 14.2×14.2 arcmin in the sky and centered approximately at the field BWC of OGLE-I: $\text{RA}(\text{J2000}) = 18^{\text{h}}03^{\text{m}}24^{\text{s}}$, $\text{DEC}(\text{J2000}) = -30^{\circ}02'00''$; (*cf.* Udalski *et al.* 1993, and also Stanek 1996) was observed on four nights between September 20 and September 25, 1998. The field overlaps in large part with BUL_SC45 field. The exposure time was 1800 seconds.

Observations collected in the drift-scan mode were reduced with the standard OGLE data pipeline and transformed to the *BVI* system based on observations of standard stars from Landolt (1992) fields collected during 5–7 photometric nights (*cf.* Udalski *et al.* 1998b). *U*-band photometry collected in the still-frame mode was reduced in similar manner as described in Udalski (1998b) with the difference that the full 2048×2048 pixel image was divided into 16 512×512 pixel sub-frames and each of them was reduced separately to ensure constant PSF. In this case transformation to the standard system was

based on photometry of standard stars collected during three photometric nights.

The systematic error of the *BVI*-band transformation should be smaller than 0.02 – 0.03 mag. For *U*-band the systematic error might be larger and we conservatively assume it to be equal to 0.05 mag. This is caused by somewhat different spectral response of the OGLE instrumental ultraviolet filter because of somewhat steeper cut of the short wavelength ($\lambda < 3500\text{\AA}$) side of the *U*-band by the telescope field corrector made from BK7 Schott glass. Nevertheless, the standard stars transform well to the standard system and the color term for *U*-band is equal to 0.127 (0.000 means the standard system) which compares to -0.041 , -0.002 and 0.029 for *B*, *V* and *I*-band, respectively.

The final list of Baade’s Window stars with *UBVI* photometry was constructed by cross-identification of all stars found in the *U*-band images with the stars from the drift-scan field BUL_SC45 using second order transformation between pixel coordinates.

Astrometric positions of stars were determined with the standard OGLE procedure as described in Udalski *et al.* (1998b). About 10270 stars from BUL_SC45 field were used to derive transformation between image pixel coordinates and the Digitized Sky Survey (DSS) coordinate system. Internal accuracy of determined equatorial coordinates is about 0.15 arcsec with possible systematic errors of the DSS system up to 0.7 arcsec.

3 *UBVI* Photometry of Baade’s Window Stars

Table 1 contains *UBVI* photometric data for 8530 stars in Baade’s Window. We provide there star ID number (in BUL_SC45 field), equatorial coordinates (J2000) and observed and extinction-free (see below) *UBVI* magnitudes of each star. Table 1 is too large to be conveniently printed, therefore only a few sample lines are shown. Full versions of Tables presented in this paper are available in electronic form from the OGLE Internet data archive: <http://www.astroww.edu.pl/~ftp/ogle> or its mirror <http://www.astro.princeton.edu/~ogle>.

The $I - (V - I)$, $I - (B - V)$, and $I - (U - B)$ color magnitude diagrams (CMDs) of Baade’s Window stars are shown in Fig. 1 for 50% of the total of 8530 stars for which *UBVI* band photometry was more accurate than 0.1 mag. The red clump is clearly visible on all three diagrams, and its width increases dramatically toward the blue and ultraviolet. For these diagrams

Table 1
UBVI photometry of 8530 stars in Baade's Window

| Star no BUL_SC45 | RA (J2000) | DEC (J2000) | U | σ_U | B | σ_B | V | σ_V | I | σ_I | U_0 | B_0 | V_0 | I_0 |
|---------------------|--|-----------------|--------|------------|--------|------------|--------|------------|--------|------------|--------|--------|--------|--------|
| 58901 | 18 ^h 03 ^m 13 ^s 32 | -30° 08' 54'' 5 | 17.590 | 0.025 | 15.468 | 0.026 | 13.689 | 0.014 | 11.792 | 0.012 | 14.660 | 13.001 | 11.839 | 10.682 |
| 58903 | 18 ^h 03 ^m 11 ^s 96 | -30° 08' 37'' 6 | 19.976 | 0.055 | 17.409 | 0.029 | 15.296 | 0.027 | 12.473 | 0.015 | 17.082 | 14.972 | 13.468 | 11.376 |
| 58904 | 18 ^h 03 ^m 12 ^s 59 | -30° 08' 34'' 1 | 19.574 | 0.025 | 17.125 | 0.052 | 15.052 | 0.061 | 11.930 | 0.050 | 16.741 | 14.739 | 13.263 | 10.856 |
| 58930 | 18 ^h 03 ^m 20 ^s 14 | -30° 08' 50'' 0 | 17.925 | 0.014 | 16.610 | 0.021 | 15.024 | 0.010 | 13.100 | 0.010 | 15.213 | 14.326 | 13.311 | 12.072 |
| 58934 | 18 ^h 03 ^m 18 ^s 49 | -30° 08' 39'' 5 | 16.441 | 0.022 | 15.866 | 0.030 | 14.818 | 0.022 | 13.565 | 0.027 | 13.746 | 13.597 | 13.116 | 12.544 |
| 58935 | 18 ^h 03 ^m 14 ^s 29 | -30° 08' 34'' 3 | 17.747 | 0.021 | 15.952 | 0.012 | 14.365 | 0.014 | 12.689 | 0.011 | 15.016 | 13.652 | 12.640 | 11.654 |
| 58936 | 18 ^h 03 ^m 19 ^s 42 | -30° 08' 34'' 5 | 20.479 | 0.084 | 18.346 | 0.024 | 16.335 | 0.028 | 12.954 | 0.013 | 17.797 | 16.087 | 14.641 | 11.938 |
| 58999 | 18 ^h 03 ^m 15 ^s 20 | -30° 08' 50'' 7 | 19.923 | 0.037 | 17.884 | 0.023 | 16.044 | 0.008 | 13.948 | 0.010 | 17.248 | 15.632 | 14.355 | 12.934 |
| 59000 | 18 ^h 03 ^m 11 ^s 04 | -30° 08' 50'' 2 | 19.223 | 0.039 | 17.536 | 0.028 | 15.914 | 0.011 | 14.137 | 0.011 | 16.222 | 15.009 | 14.019 | 13.000 |
| 59001 | 18 ^h 03 ^m 18 ^s 83 | -30° 08' 48'' 8 | 15.904 | 0.010 | 15.728 | 0.015 | 15.066 | 0.009 | 14.193 | 0.009 | 13.199 | 13.450 | 13.358 | 13.168 |
| 59002 | 18 ^h 03 ^m 12 ^s 46 | -30° 08' 42'' 3 | 16.464 | 0.003 | 16.029 | 0.013 | 15.103 | 0.017 | 13.912 | 0.011 | 13.544 | 13.570 | 13.259 | 12.805 |
| 59003 | 18 ^h 03 ^m 19 ^s 52 | -30° 08' 42'' 0 | 15.481 | 0.001 | 15.276 | 0.016 | 14.844 | 0.013 | 14.236 | 0.008 | 12.775 | 12.997 | 13.135 | 13.211 |
| 59174 | 18 ^h 03 ^m 14 ^s 44 | -30° 08' 45'' 3 | 20.348 | 0.089 | 19.494 | 0.087 | 17.178 | 0.059 | 15.253 | 0.016 | 17.575 | 17.158 | 15.426 | 14.202 |
| 59175 | 18 ^h 03 ^m 09 ^s 10 | -30° 08' 44'' 1 | 21.456 | 0.023 | 19.085 | 0.050 | 17.187 | 0.021 | 15.132 | 0.012 | 18.402 | 16.514 | 15.258 | 13.975 |
| 59176 | 18 ^h 03 ^m 04 ^s 49 | -30° 08' 40'' 6 | 19.844 | 0.060 | 18.611 | 0.030 | 17.137 | 0.071 | 15.243 | 0.021 | 16.922 | 16.150 | 15.291 | 14.136 |
| 59177 | 18 ^h 03 ^m 14 ^s 35 | -30° 08' 41'' 0 | 21.223 | 0.098 | 18.762 | 0.033 | 16.946 | 0.011 | 15.041 | 0.011 | 18.459 | 16.434 | 15.200 | 13.993 |
| 59178 | 18 ^h 03 ^m 13 ^s 91 | -30° 08' 39'' 6 | 17.426 | 0.013 | 16.765 | 0.021 | 15.818 | 0.013 | 14.713 | 0.015 | 14.622 | 14.404 | 14.047 | 13.650 |
| 59180 | 18 ^h 03 ^m 10 ^s 00 | -30° 08' 33'' 7 | 16.719 | 0.007 | 16.356 | 0.014 | 15.660 | 0.021 | 14.631 | 0.020 | 13.707 | 13.819 | 13.757 | 13.489 |
| 59494 | 18 ^h 03 ^m 07 ^s 90 | -30° 08' 51'' 8 | 20.342 | 0.007 | 19.215 | 0.055 | 17.806 | 0.018 | 16.121 | 0.020 | 17.298 | 16.651 | 15.883 | 14.967 |

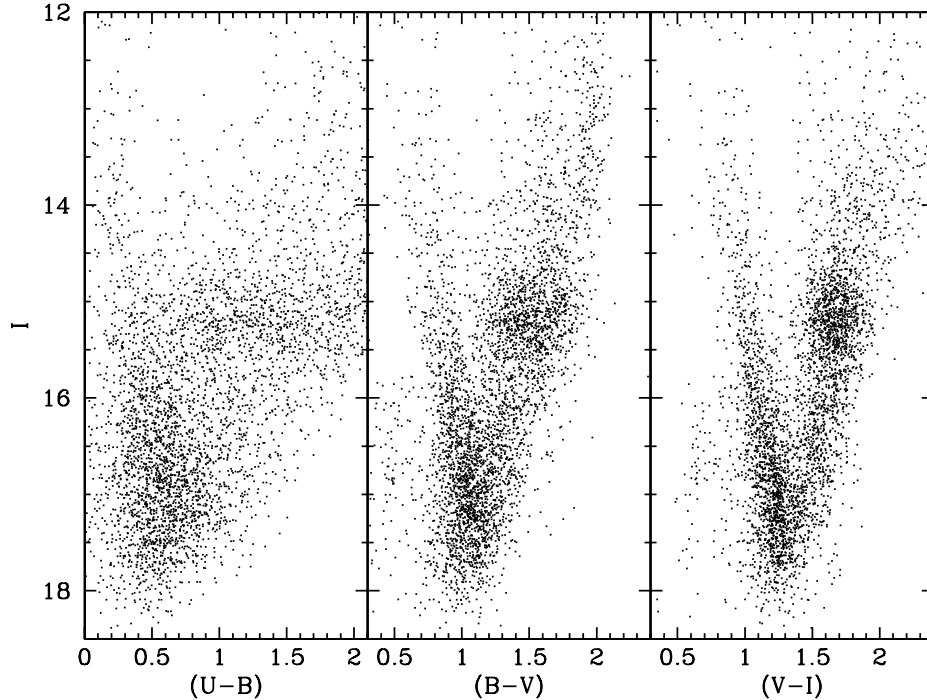


Fig. 1. Color-magnitude diagrams for 50% of the 8530 stars in Baade's Window for which *UBVI* photometry was obtained by the OGLE-II. Photometric errors in all bands are smaller than 0.1 mag. Notice the increase of color range of red clump giants progressing from $(V-I)$, through $(B-V)$ to $(U-B)$.

to be useful we have to correct them for interstellar reddening.

4 Reddening Map

We followed Kiraga, Paczyński and Stanek (1997) in the determination of interstellar reddening variation over our field. We selected 38,249 stars for which *V* and *I*-band photometry was more accurate than 0.1 mag. The corresponding CMD for 25% of those stars is shown in Fig. 2. Four regions were selected: one near the red clump (RC), one below it, at the red giant branch (RG), and two near the main sequence turn off point, one brighter, and the other one fainter (TOPb, TOPf), as indicated in Fig. 2. The six parallel lines are described with the equations: $I - 1.5 \times (V - I) = C$, where

$C=12.00, 13.25, 14.50, 15.50, 16.00, 16.50$, respectively. The slope of these lines was chosen so that they are parallel to the reddening vector (Stanek 1996).

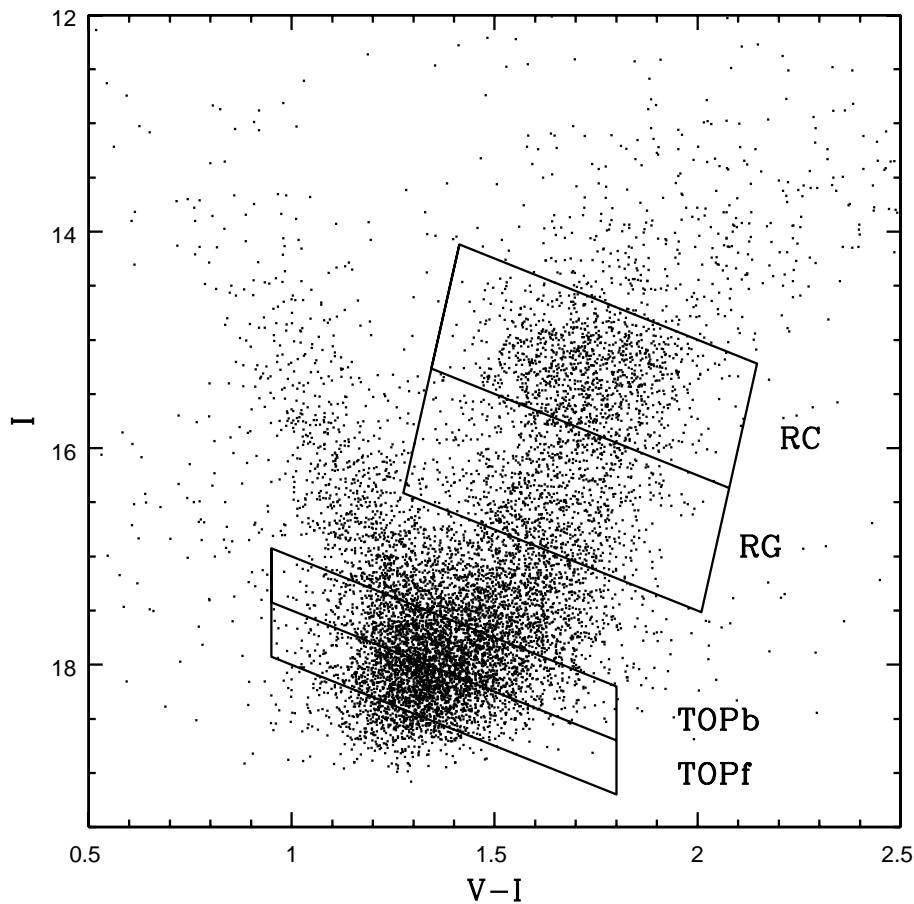


Fig. 2. Color-magnitude diagram for 25% of the 38,249 stars in Baade's Window for which V and I -band photometry was obtained by the OGLE-II. Photometric errors in both bands are smaller than 0.1 mag. The stars in the four marked regions were used for reddening determination.

We divided our field into squares of 200×200 pixels. In every square we calculated average color of the stars in each of the four groups separately, and also the average of the stars in all four groups. It is safe to assume that there was no significant variation in stellar populations within our field, which had the total area of only $(0.23)^2$. The variation of average colors

was due to variation in the interstellar reddening as well as the statistical fluctuations caused by a small number of stars.

The colors of all four stellar groups are very well correlated, as shown in Fig. 3. To bring the colors of the four groups to the same average value the corrections were added to the $(V-I)$ color of each star, with $\Delta(V-I)_{TOPf} = +0.200$ mag, $\Delta(V-I)_{TOPb} = +0.138$ mag, $\Delta(V-I)_{RG} = -0.120$ mag and $\Delta(V-I)_{RC} = -0.217$ mag. The shift between colors of each group in Fig. 3 has been increased for the clarity of presentation.

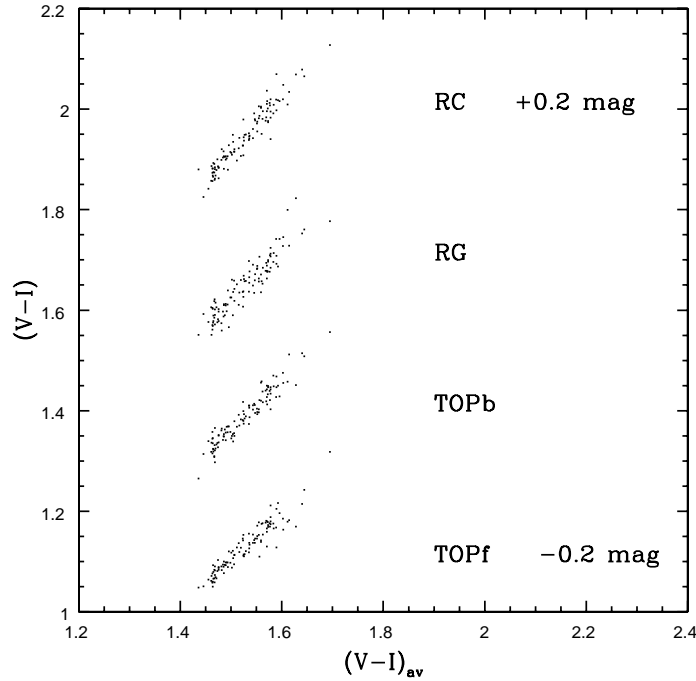


Fig. 3. The relation between the average $(V-I)$ colors of the stars in four areas indicated in Fig. 2 are shown as a function of the average $(V-I)_{av}$ for stars in all four areas. Each dot corresponds to a different square in the CCD field, 200×200 pixels, *i.e.*, $83''.4 \times 83''.4$ each.

As there was such a good correlation between the colors of the four groups we combined all stars, adding the suitable corrections as given above. We calculated average colors for the stars in squares 50×50 pixels, *i.e.*, $20''.8 \times 20''.8$ in the sky. The total number of such squares in our field was $39 \times 42 = 1638$. These became our resolution elements for the reddening map, or the elementary squares. The number of stars in the four groups was: $N_{TOPf} = 6422$, $N_{TOPb} = 7776$, $N_{RG} = 4185$, $N_{RC} = 4546$. The total number

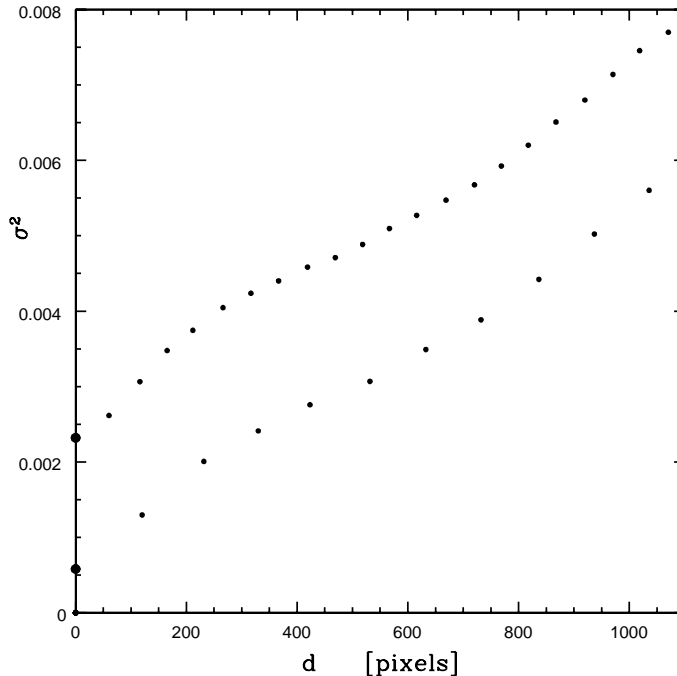


Fig. 4. The two correlation functions σ^2 of the variation in the $(V-I)$ is shown as a function of separation d . The upper sequence of points corresponds to the resolution 50×50 pixels, while the lower sequence corresponds to the resolution 100×100 pixels.

of all stars used for the reddening determination was $N=22,929$, the average number of stars per elementary square was $n=14.0$, and the variance of the average color was $\langle \sigma_{V-I}^2 \rangle = (0.034 \text{ mag})^2$. The *rms* variation of the $(V-I)$ color per star was approximately 0.13 mag.

Given the values of the average $(V-I)$ colors in 1638 elementary squares we calculated the correlation function defined as

$$\sigma^2(d) = \langle \Delta(V-I)^2 \rangle, \quad (1)$$

averaged over all pairs of squares within each range of separations d . σ^2 is shown in Fig. 4 as a function of the separation between the elementary squares (the upper sequence of points). The point corresponding to the separation $d=0$ is twice the variance of the $(V-I)$ color per elementary square. Fig. 4 shows that the value of the correlation function doubles at a separation $d \approx 500$ pixels, which is 10 times larger than the elementary square size. We repeated the exercise by combining 4 adjacent elementary squares

into one composite square of 100×100 pixels, thereby increasing the average number of stars to 56.0, and reducing the variance of the average $(V - I)$ color to $(0.017 \text{ mag})^2$. The corresponding correlation points are shown as the lower sequence in Fig. 4. This time the correlation function doubles its value at a separation $d \approx 100$ pixels.

While the zero point depends on the choice of the square size, the rest of the correlation function is the same in both cases, except for the zero point shift. The contribution of interstellar reddening to the correlation function may be approximated as

$$\langle \Delta E_{V-I}^2 \rangle \approx (0.027 \text{ mag})^2 \times \frac{d}{1'}, \quad 0 < d < 7'. \quad (2)$$

How to choose the right square size? If the squares are small then the resolution is high, and the variations of interstellar reddening from square to square are small. However, there are few stars per square and the statistical error in the estimate of the average stellar color is large. When the squares are large the opposite is true: the average color is calculated accurately, but the resolution is poor and the variations of the interstellar reddening within the square become substantial. Without attempting a rigorous analysis it seems that a sensible square size is such, that the two contributions: the random noise due to a finite number of stars within the square, and the variations of the interstellar reddening within the square are comparable. Fig. 4 suggests that a sensible choice is a square size 100×100 pixels, i.e. $41''.7 \times 41''.7$ in the sky.

We calculated average $(V - I)_{av}$ color for the stars in a grid of 100×100 pixel squares. We shifted the grid by 50 pixels in both directions, so as to have average color calculated at 50 pixel intervals. A comparison between the $(V - I)_{av}$ color from our data and the color excess E_{V-I} calculated with the Stanek's (1996) extinction map is shown in Fig. 5. The agreement is good, and we adopt the relation:

$$E_{V-I} = (V - I)_{av} - 0.931, \quad \langle E_{V-I} \rangle = 0.59. \quad (3)$$

Obviously, our method, as well as Stanek's, provides only a differential reddening map. The zero point adopted by Stanek, and therefore also by us, is based on the determination by Gould *et al.* (1998) and Alcock *et al.* (1998).

We calculate reddening within our $(0.23^\circ)^2$ field by linear interpolation in the grid with the spacing of 50 pixels. The values of E_{V-I} are based on the average $(V - I)_{av}$ calculated in 100×100 pixel squares. Therefore,

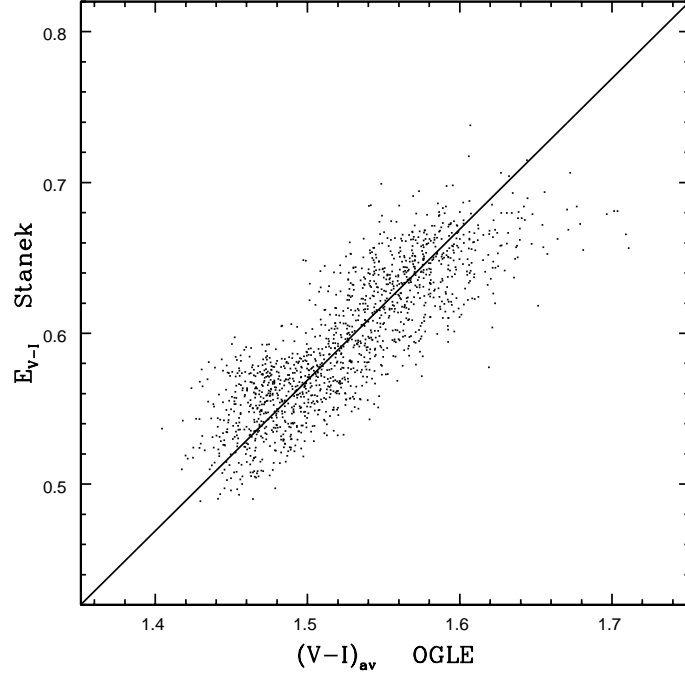


Fig. 5. The correlation of the average color $(V-I)_{av}$ of the OGLE stars on the reddening E_{V-I} calculated with Stanek's (1996) map. The diagonal line is the relation: $(V-I)_{av} = E_{V-I} + 0.931$.

the resolution of our extinction map is 100 pixels, *i.e.*, $41''7$ in the sky. We estimate the statistical accuracy of our reddening map to be ≈ 0.02 mag. Of course, the uncertainty in the zero point of our extinction is substantially larger. The FORTRAN code RED.F, calculating reddening within our field is available from the OGLE Internet archive.

5 Color–Color Diagrams

The extinction in the four bands was calculated according to the formulae:

$$A_I = 1.500 \cdot E_{V-I}, \quad \langle A_I \rangle = 0.88, \quad (4a)$$

$$A_V = 2.500 \cdot E_{V-I}, \quad \langle A_V \rangle = 1.48, \quad (4b)$$

$$A_B = 3.333 \cdot E_{V-I}, \quad \langle A_B \rangle = 1.97, \quad (4c)$$

$$A_U = 3.958 \cdot E_{V-I}, \quad \langle A_U \rangle = 2.34, \quad (4d)$$

and the colors were corrected for the reddening accordingly. The reddening varied relatively little over our small field of view, with 90% of stars in the range $0.51 < E_{V-I} < 0.65$. Therefore, the CMDs corrected for extinction were similar to those shown in Fig. 1, except for a shift in color and magnitude.

To facilitate follow-up observations of the red clump giants we selected stars from Table 1 according to the following criteria:

$$14.0 < I_0 < 14.7, \quad 0.8 < (V - I)_0 < 1.6, \quad \text{errors} < 0.05 \text{ mag.} \quad (5)$$

640 stars satisfied these criteria. They, and the relevant data, are listed in Table 2 (full version is available from the OGLE Internet archive).

We also selected red clump giants from the Hipparcos catalog according to the following criteria: genuine I -band photometry was available in the catalog, the absolute magnitude M_I , the color $(V - I)$, and the parallax π satisfied the criteria:

$$-0.5 < M_I < 0.2, \quad 0.8 < (V - I) < 1.6, \quad \pi \text{ error} < 10\%, \quad (6)$$

J-C. Mermilliod kindly provided us with the UBV photometry for the selected stars in a computer readable form (*cf.* Mermilliod and Mermilliod 1994, and <http://obswww.unige.ch/gcpd/>). The list of 309 stars which satisfied the criteria given above, had $UBVI$ photometry and had the differences in V and B magnitudes as given by the Hipparcos/Tycho catalogs and by Mermilliod not larger than 0.03 mag, are listed in Table 3 (full version is available from the OGLE Internet archive). The coordinates in Table 3 are for J2000, which is based on the Hipparcos' epoch J1991.25, with the correction due to precession taken into account, but with no allowance for the stellar proper motion. As all Hipparcos stars with accurate parallaxes are within 100 pc, their reddening is very small (Stanek and Garnavich 1998, Sekiguchi and Fukugita 1999).

The number of red clump giants for which Hipparcos provides accurate parallaxes is several times larger than 309, and they all have accurate V and B photometry, but a large fraction does not have either I or U data. The calibration of red clump giants could be improved considerably if standard I and U photometry were made for these bright stars.

Figs. 6 and 7 show $(V - I)_0 - (B - V)_0$ and $(B - V)_0 - (U - B)_0$ color-color diagrams constructed for 640 Baade's Window red clump giants. Figs. 8 and 9 show similar diagrams for the Hipparcos sample of red clump stars.

Table 2
UBVI photometry of 640 red clump giants in Baade's Window

| Star no BUL_SC45 | RA (J2000) | DEC (J2000) | U | σ_U | B | σ_B | V | σ_V | I | σ_I | U_0 | B_0 | V_0 | I_0 |
|---------------------|--|-----------------|--------|------------|--------|------------|--------|------------|--------|------------|--------|--------|--------|--------|
| 67593 | 18 ^h 03 ^m 16 ^s 02 | -30° 07' 15'' 9 | 20.629 | 0.050 | 18.570 | 0.050 | 16.812 | 0.011 | 15.031 | 0.008 | 18.156 | 16.487 | 15.250 | 14.094 |
| 67598 | 18 ^h 03 ^m 12 ^s 28 | -30° 07' 12'' 7 | 18.681 | 0.020 | 17.930 | 0.024 | 16.623 | 0.016 | 15.076 | 0.009 | 16.256 | 15.888 | 15.092 | 14.157 |
| 67616 | 18 ^h 03 ^m 16 ^s 78 | -30° 06' 57'' 9 | 20.316 | 0.012 | 18.604 | 0.040 | 16.996 | 0.013 | 15.226 | 0.015 | 17.829 | 16.510 | 15.425 | 14.284 |
| 67617 | 18 ^h 03 ^m 13 ^s 92 | -30° 06' 56'' 5 | 18.784 | 0.014 | 18.152 | 0.047 | 16.550 | 0.017 | 15.020 | 0.018 | 16.373 | 16.121 | 15.027 | 14.106 |
| 67627 | 18 ^h 03 ^m 12 ^s 27 | -30° 06' 48'' 8 | 19.701 | 0.037 | 18.683 | 0.020 | 17.100 | 0.010 | 15.441 | 0.015 | 17.266 | 16.632 | 15.562 | 14.518 |
| 67641 | 18 ^h 03 ^m 13 ^s 40 | -30° 06' 38'' 1 | 20.102 | 0.041 | 18.619 | 0.026 | 16.957 | 0.013 | 15.160 | 0.009 | 17.669 | 16.570 | 15.420 | 14.238 |
| 67657 | 18 ^h 03 ^m 19 ^s 34 | -30° 06' 24'' 2 | 19.724 | 0.023 | 18.223 | 0.037 | 16.686 | 0.013 | 14.958 | 0.009 | 17.230 | 16.123 | 15.111 | 14.013 |
| 67663 | 18 ^h 03 ^m 11 ^s 03 | -30° 06' 20'' 4 | 19.931 | 0.014 | 18.475 | 0.021 | 16.943 | 0.017 | 15.264 | 0.010 | 17.588 | 16.502 | 15.463 | 14.376 |
| 67673 | 18 ^h 03 ^m 11 ^s 81 | -30° 06' 15'' 0 | 19.098 | 0.009 | 18.131 | 0.024 | 16.783 | 0.011 | 15.229 | 0.011 | 16.804 | 16.199 | 15.334 | 14.360 |
| 67680 | 18 ^h 03 ^m 10 ^s 90 | -30° 06' 09'' 0 | 19.332 | 0.032 | 18.190 | 0.038 | 16.761 | 0.018 | 15.139 | 0.011 | 16.999 | 16.225 | 15.287 | 14.255 |
| 67686 | 18 ^h 03 ^m 14 ^s 39 | -30° 06' 03'' 6 | 19.324 | 0.024 | 18.099 | 0.023 | 16.686 | 0.006 | 15.084 | 0.008 | 16.923 | 16.077 | 15.169 | 14.174 |
| 67695 | 18 ^h 03 ^m 07 ^s 57 | -30° 05' 57'' 4 | 18.837 | 0.010 | 18.095 | 0.023 | 16.769 | 0.014 | 15.149 | 0.011 | 16.228 | 15.898 | 15.121 | 14.160 |
| 67701 | 18 ^h 03 ^m 13 ^s 04 | -30° 05' 53'' 2 | 19.352 | 0.028 | 18.213 | 0.024 | 16.838 | 0.010 | 15.282 | 0.016 | 17.051 | 16.276 | 15.385 | 14.410 |
| 67712 | 18 ^h 03 ^m 04 ^s 25 | -30° 05' 43'' 9 | 19.822 | 0.047 | 18.446 | 0.040 | 16.869 | 0.014 | 15.111 | 0.019 | 17.180 | 16.221 | 15.200 | 14.110 |
| 67718 | 18 ^h 03 ^m 10 ^s 29 | -30° 05' 40'' 1 | 20.036 | 0.037 | 18.379 | 0.046 | 16.827 | 0.017 | 15.080 | 0.013 | 17.572 | 16.304 | 15.271 | 14.146 |
| 67724 | 18 ^h 03 ^m 13 ^s 83 | -30° 05' 36'' 1 | 19.511 | 0.019 | 18.380 | 0.028 | 16.953 | 0.011 | 15.299 | 0.014 | 17.156 | 16.397 | 15.465 | 14.406 |
| 67733 | 18 ^h 03 ^m 14 ^s 52 | -30° 05' 27'' 1 | 19.379 | 0.041 | 18.169 | 0.028 | 16.735 | 0.015 | 15.087 | 0.017 | 16.974 | 16.144 | 15.216 | 14.176 |
| 67736 | 18 ^h 03 ^m 10 ^s 97 | -30° 05' 23'' 2 | 20.170 | 0.043 | 18.658 | 0.050 | 17.168 | 0.021 | 15.466 | 0.016 | 17.758 | 16.627 | 15.645 | 14.552 |
| 67744 | 18 ^h 03 ^m 17 ^s 25 | -30° 05' 20'' 1 | 19.211 | 0.021 | 18.181 | 0.027 | 16.826 | 0.016 | 15.208 | 0.023 | 16.713 | 16.078 | 15.248 | 14.261 |

Table 3
Hipparcos red clump giants

| Hipparcos no | RA (J2000) | DEC (J2000) | $(V - I)$ | $(B - V)$ | $(U - B)$ | V | M_V | M_I | d [pc] |
|-----------------|--|-----------------|-----------|-----------|-----------|-------|-------|--------|-------------|
| 671 | 0 ^h 08 ^m 44 ^s .39 | -8° 46' 31.''3 | 0.990 | 1.035 | 0.828 | 5.985 | 0.944 | -0.046 | 102.14 |
| 765 | 0 ^h 09 ^m 50 ^s .94 | -45° 41' 54.''0 | 1.000 | 1.024 | 0.843 | 3.872 | 0.715 | -0.285 | 42.96 |
| 814 | 0 ^h 10 ^m 25 ^s .36 | -82° 10' 31.''2 | 0.980 | 1.050 | 0.925 | 5.268 | 0.934 | -0.046 | 74.35 |
| 966 | 0 ^h 12 ^m 22 ^s .47 | -42° 07' 24.''2 | 1.010 | 1.040 | 0.840 | 6.530 | 1.037 | 0.027 | 125.47 |
| 2568 | 0 ^h 33 ^m 02 ^s .92 | 20° 20' 33.''5 | 1.000 | 1.069 | 0.956 | 5.367 | 0.897 | -0.103 | 78.80 |
| 2926 | 0 ^h 37 ^m 34 ^s .95 | 24° 03' 44.''3 | 1.080 | 1.179 | 1.269 | 6.171 | 1.125 | 0.045 | 102.56 |
| 3031 | 0 ^h 39 ^m 01 ^s .51 | 29° 21' 37.''4 | 0.920 | 0.871 | 0.466 | 4.360 | 0.772 | -0.148 | 51.71 |
| 3092 | 0 ^h 39 ^m 47 ^s .70 | 30° 54' 33.''1 | 1.230 | 1.279 | 1.484 | 3.263 | 0.809 | -0.421 | 31.07 |
| 3137 | 0 ^h 40 ^m 16 ^s .80 | -44° 44' 54.''1 | 1.060 | 1.144 | 1.090 | 6.005 | 1.157 | 0.097 | 93.02 |
| 3455 | 0 ^h 44 ^m 37 ^s .88 | -10° 33' 41.''3 | 0.980 | 1.015 | 0.843 | 4.756 | 0.727 | -0.253 | 64.35 |
| 3456 | 0 ^h 44 ^m 37 ^s .03 | -38° 22' 27.''1 | 1.070 | 1.142 | 1.181 | 5.877 | 0.613 | -0.457 | 114.15 |
| 3781 | 0 ^h 48 ^m 52 ^s .88 | -74° 52' 32.''7 | 1.340 | 1.368 | 1.674 | 5.061 | 1.102 | -0.238 | 62.74 |
| 4257 | 0 ^h 54 ^m 44 ^s .06 | -8° 41' 35.''6 | 0.910 | 0.916 | 0.533 | 6.163 | 0.822 | -0.088 | 116.28 |
| 4422 | 0 ^h 57 ^m 11 ^s .73 | 59° 13' 42.''2 | 1.010 | 0.955 | 0.679 | 4.627 | 0.619 | -0.391 | 63.13 |
| 4587 | 0 ^h 59 ^m 10 ^s .19 | -11° 19' 58.''2 | 0.960 | 0.942 | 0.672 | 5.618 | 0.695 | -0.265 | 96.62 |
| 5170 | 1 ^h 06 ^m 33 ^s .15 | -23° 56' 44.''5 | 1.020 | 1.079 | 1.002 | 6.137 | 0.965 | -0.055 | 107.41 |
| 5364 | 1 ^h 09 ^m 01 ^s .54 | -10° 08' 07.''5 | 1.110 | 1.161 | 1.190 | 3.441 | 0.675 | -0.435 | 36.06 |
| 5485 | 1 ^h 10 ^m 38 ^s .31 | -8° 51' 34.''6 | 0.980 | 1.032 | 0.880 | 6.391 | 1.157 | 0.177 | 111.86 |
| 5586 | 1 ^h 12 ^m 08 ^s .58 | 30° 08' 09.''8 | 1.050 | 1.092 | 1.011 | 4.509 | 1.027 | -0.023 | 49.73 |

6 Discussion

6.1 *UBVI* Observations

The data we present in this paper cannot by itself resolve the current ambiguity about the relation between the colors and the metallicity of red clump giants (Paczynski 1998). However, the catalogs of these stars in Baade's Window (Table 2) and near the Sun (Table 3) can be used to select stars over the full range of colors for spectroscopic studies.

The tight color-color relations apparent for the Hipparcos stars (Figs. 8 and 9) clearly indicate that either there is a single parameter that determines the red clump colors, or there is a degeneracy between several parameters, which conspire to change stellar colors in the same direction in the three dimensional space of $(V - I) - (B - V) - (U - B)$. The same appears to be true for the red clump giants in Baade's Window (Figs. 6 and 7). The scatter is larger in Baade's Window for at least two reasons: photometric errors are larger than for the bright Hipparcos stars, and reddening corrections are not perfect. It is somewhat disturbing that the slope of the $(B - V)_0 - (V - I)_0$ relation is somewhat different for the stars in Baade's Window than those near the Sun. In principle there is a possibility that the reddening vector varies significantly with the stellar color, but we did not make an estimate of this effect.

If future spectroscopic determinations of the metallicity establish only a weak correlation with colors of red clump giants, then it will be clear that another parameter, most likely the mass (i.e. age) of a star affects its colors too. This would imply that red clump giants make large loops in the CMD during their core helium burning phase. However, if it turns out that the spectroscopic metallicity is very well correlated with colors, then the implication will be that the dependence on mass (age) is weak, and the evolutionary loops are small.

Note, that our samples of the red clump giants are not likely to be biased by their colors, as they are all well above the detection limit.

Following the approach of Paczynski and Stanek (1998) we determined that the number density of red clump stars peaks at $I_0 = 14.37 \pm 0.02$. Of course, the true error may be as large as 0.1 mag because the zero point of the interstellar extinction is uncertain (Alcock *et al.* 1998, Gould *et al.* 1998).

Stanek *et al.* (1999) have presented *UBVI* photometry in a nearby field BW8 in Baade's Window. Their results are in substantial agreement with

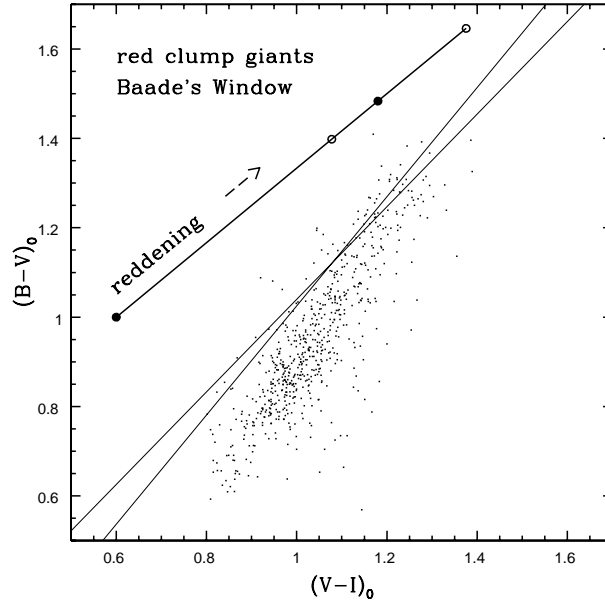


Fig. 6. The color – color diagram: $(V-I)_0 - (B-V)_0$ for 640 red clump giants in Baade's Window, with the photometric errors smaller than 0.05 mag, corrected for interstellar reddening. The two thin lines that cross are for reference; they are the same as in Fig. 8.

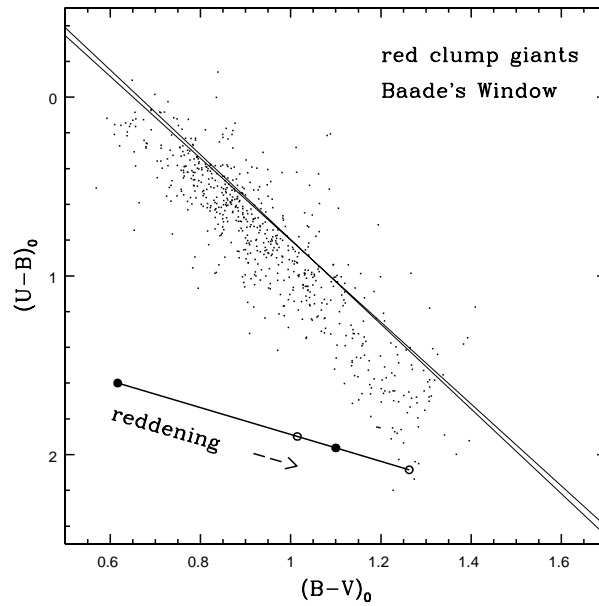


Fig. 7. The color – color diagram: $(B-V)_0 - (U-B)_0$ for 640 red clump giants in Baade's Window, with the photometric errors smaller than 0.05 mag, corrected for interstellar reddening. The two thin lines that cross are for reference; they are the same as in Fig. 9.

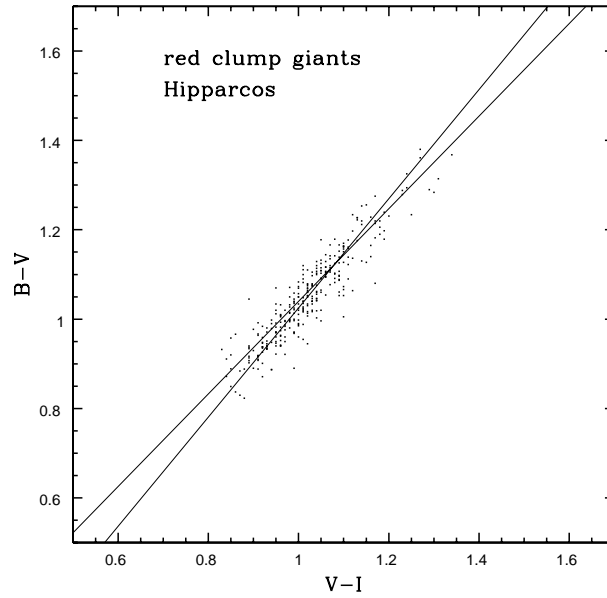


Fig. 8. The color – color diagram: $(V - I) - (B - V)$ for 309 red clump giants for which Hipparcos measured parallaxes with the accuracy better than 10%. The two thin lines that cross are the regression lines of one color with respect to another.

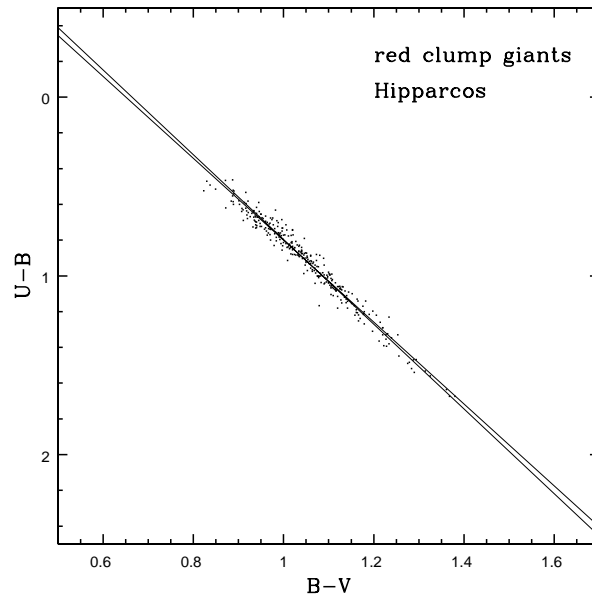


Fig. 9. The color – color diagram: $(B - V) - (U - B)$ for 309 red clump giants for which Hipparcos measured parallaxes with the accuracy better than 10%. The two thin lines that cross are the regression lines of one color with respect to another.

ours, although there appear to be some systematic differences of order of 0.05 mag in zero points of photometry. They also discuss the effect of metallicity on colors of the red clump stars.

6.2 Stellar Models

It is remarkable how well the models of red clump giants agree with the observations. Recently, evolutionary tracks for a broad range of metallicities and masses were calculated by Bertelli *et al.* (1994), Jimenez, Flynn and Kotoneva (1998), and by Girardi *et al.* (1998). The results are best summarized by Fig. 1 of Girardi *et al.* (1998), which clearly shows that the absolute *I*-band magnitude changes very little with stellar mass (*i.e.*, age), but it increases by 0.2–0.3 mag when the metallicity decreases from $Z=0.03$ to $Z=0.001$, in a fairly good agreement with the Udalski's (1998b) empirical calibration. Models demonstrate that while the metallicity is the dominant factor affecting the colors, the stellar mass (age) makes a non-negligible contribution, especially at high metallicities, where red clump giants make fairly large horizontal loops in the CMD. This suggests that there is some degeneracy, in the sense that metallicity and stellar mass (age) move a star along nearly the same, approximately horizontal vector in the CMD, and along approximately the same vector in a color–color diagram.

Things are different at very low metallicities, like those found in Leo I (Caputo *et al.* 1999), where $Z=0.0004$ or even 0.0001. Under these extreme conditions the red clump appears like a small arc, with the top and bottom relatively blue, and the middle relatively red. The range of luminosities of the red clump giants in Leo I is larger than the range observed in the Galaxy (*e.g.*, Paczyński and Stanek 1998), Magellanic Clouds (*e.g.*, Udalski *et al.* 1998a, Stanek, Zaritsky and Harris 1998), or in M31 (Stanek and Garnavich 1998). This is in excellent agreement with the prediction of stellar evolutionary models (Bertelli *et al.* 1994), and indicates a very large spread in masses (ages) of the extremely metal poor population observed in Leo I (Caputo *et al.* 1999).

Things are also different for very young red clump giants, as it is apparent in the data (Udalski *et al.* 1998a) and in the models (*cf.* Fig. 1 of Girardi *et al.* 1998): the stars younger than 2 Gyr are brighter than those in the age group of 2–10 Gyr. However, it is remarkable, that in all objects with a large number of red clump giants that were studied so far: Hipparcos stars and the Galactic bulge (Paczyński and Stanek 1998), LMC, SMC, Carina dwarf galaxy (Udalski *et al.* 1998a, Udalski 1998a), M31 (Stanek and Garnavich

1998), the red clump shows very little spread in the I -band magnitude, indicating that the stellar population is dominated by stars which are 2–10 Gyr old.

While one may argue about 0.1 mag or even 0.2 mag discrepancy between the models and the observations (*e.g.*, Girardi 1999), it is comparable to, or better than, the situation with the RR Lyrae stars or with Cepheids, except those stars do not have empirical calibration as good as the red clump giants. A thorough comparison between the models and the data for the red clump giants can be found in Stanek *et al.* (1999).

While the evolutionary models are in a reasonable agreement with the observations, one should be aware of several problems with the models which cannot be readily resolved and which make a perfect agreement with the data almost impossible.

It is well known that theory cannot predict what should be the value of the mixing length parameter which is used to describe non-adiabatic convection below stellar photosphere. Moreover, the model effective temperature and radius are very sensitive to this parameter, and in practice the calibration is empirical. However, there is no reason for the mixing length parameter to be a universal constant, and today's theory cannot make a firm prediction of the effective temperature of any cool star, including red clump giants.

In order to be compared with the observations the effective temperature of a stellar model is converted to a color, like $(V - I)$, which introduces next theoretical step: model atmosphere. While these are ever more sophisticated and presumably accurate, ultimately the accuracy of the T_{eff} vs. color transformation has to be empirically verified. The same is true for the bolometric corrections. Note that the bolometric luminosity provided by stellar models is not sensitive to the value of mixing length parameter. However, the bolometric correction rests on model atmospheres and their empirical calibration.

Stochastic mass loss from red giant stars is believed to be responsible for the morphology of the horizontal branch (Rood 1973, Chiosi, Bertelli, and Bressan 1992). In other words, the amount of matter lost affects stellar radius and effective temperature, affecting the size of a loop the star makes in the CMD. Red clump giants have identical interior structure as classical horizontal branch stars and therefore their loops are also affected by the amount of mass loss. As the reason for the stochastic nature of mass loss is not known, the size of those loops cannot be firmly predicted by the theory.

There is yet another major uncertainty of the models, which is not very

well known, or not very well remembered. Several decades ago it was established that low mass stars develop large semiconvective zones just outside of their convective helium burning cores (Schwarzschild 1970, Iben 1974, and references therein). The question: ‘what is the proper criterion for a marginally stable gradient of chemical composition’ was debated. There has been no discussion of this subject lately, and there is no reference to the semiconvection in recent papers on models of horizontal branch or red clump stars. It is not clear whether the problem has been solved or forgotten.

Another very delicate issue is the extent to which chemical composition profile affects the size of the loops that stars make in the CMD while burning helium in their cores. Robertson (1971), and Lauterborn, Refsdal, and Weigert (1971) demonstrated that even very small changes in the stellar interior had a huge effect on the loop size. This is not important when the red clump models are very close to the red giant branch, i.e. when the loop is very small, and the range of colors is very small. However, high metallicity clump models appear to have fairly extended loops (*cf.* Fig. 1 of Girardi *et al.* 1998), and the size of these may be very sensitive to many details of stellar structure.

The issue of the loop size can be most reliably resolved with the spectral observations, which may establish how tight (or not tight) is the correlation between the colors and metallicity of the red clump giants. The tighter the correlation, the smaller the loops have to be, and vice versa.

Considering the many difficulties with the stellar models it is not likely that they can provide quantities like M_I and $(V-I)_0$ with a precision better than 0.1 – 0.2 mag, unless empirically calibrated. This is roughly the level at which the models and the observations appear to agree or disagree with each other.

6.3 Red Clump in the SMC

Although the Small Magellanic Cloud is not the topic of this paper, we present in Fig. 10 a color magnitude diagram for the red clump for a region near the south-west end of the SMC bar. We took the data from the SMC Photometric Maps published by the OGLE team (Udalski *et al.* 1998b), which have been accessible from the OGLE archive for over a year. The main reason for presenting Fig. 10 is to show how compact the red clump is when the reddening is not a problem, the range of distances is small, and the range of metallicities is low too. The data from the SMC maps may be useful to test and/or calibrate theoretical models. In particular, it is

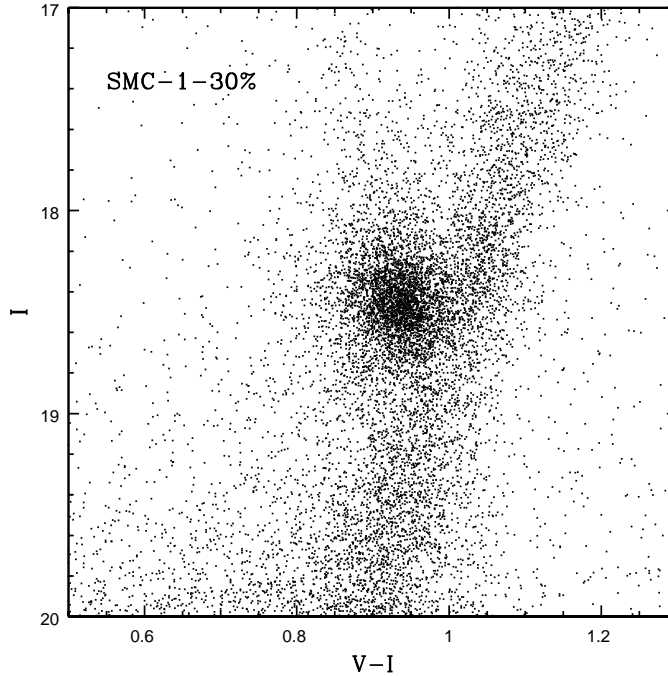


Fig. 10. Color-magnitude diagram for 30% of stars in the SMC field SMC_LSC1 (Udalski *et al.* 1998b). Note how narrow is the red giant branch and how compact is the red clump in this field with low and uniform reddening.

striking that the red clump in the SMC has no apparent structure, except for a cloud of stars above the main body of the clump; these are likely the younger and more massive stars as shown in Fig. 1 of Girardi *et al.* (1998).

Acknowledgments. It is a great pleasure to acknowledge numerous discussions with Dr. K. Z. Stanek. We are very indebted to Dr. J.-C. Mermilliod for providing us with the *UBV* data for the Hipparcos stars in a computer readable form. This work was supported with the NSF grants AST-9530478 and AST-9820314 to B. Paczyński and the Polish KBN grant 2P03D00814 to A. Udalski.

REFERENCES

- Alcock, C. et al. 1998, *Astrophys. J.*, **494**, 396.
 Bertelli, G. et al. 1994, *Astron. Astrophys. Suppl. Ser.*, **106**, 275.
 Caputo, F. et al. 1999, *Astron. J.*, **117**, 2199.

- Chiosi, C., Bertelli, G., and Bressan, A. 1992, *ARAA*, **30**, 235.
- Girardi, L., Groenewegen, M. A. T, Weiss, A., and Salaris, M. 1998, *MNRAS*, **301**, 149.
- Girardi, L. 1999, astro-ph/9807086.
- Gould, A., Popowski, P., and Terndrup, D. M. 1998, *Astrophys. J.*, **492**, 778.
- Horner, D. et al. 1999, astro-ph/9907213.
- Iben, I. Jr. 1974, *ARAA*, **12**, 215.
- Jimenez, R., Flynn, C., and Kotoneva, E. 1998, *MNRAS*, **299**, 515.
- Kiraga, M., Paczyński, B., and Stanek, K.Z. 1997, *Astrophys. J.*, **485**, 611.
- Landolt, A.U. 1992, *Astron. J.*, **104**, 372.
- Lauterborn, D., Refsdal, S., and Weigert, A. 1971, *Astron. Astrophys.*, **10**, 97.
- Mermilliod, J.-C., and Mermilliod, M. 1994, *Catalogue of Mean *UBV* Data on Stars*, Springer-Verlag.
- Paczyński, B. 1998, *Acta Astron.*, **48**, 405.
- Paczyński, B., and Stanek, K.Z. 1998, *Astrophys. J. Letters*, **494**, L219.
- Perryman, M. A. C. et al. 1997, *Astron. Astrophys.*, **323**, L49.
- Robertson, J. W. 1971, *Astrophys. J.*, **164**, L105.
- Rood, R. T. 1973, *Astrophys. J.*, **184**, 815.
- Schwarzschild, M. 1970, *Quart. J. RAS*, **11**, 12.
- Sekiguchi, M., and Fukugita, M. 1999, astro-ph/9904299.
- Stanek, K. Z. 1996, *Astrophys. J.*, **460**, L37.
- Stanek, K. Z. and Garnavich, P. M. 1998, *Astrophys. J.*, **503**, 131.
- Stanek, K. Z., Zaritsky, D., and Harris, J. 1998, *Astrophys. J.*, **500**, 141.
- Stanek, K. Z., Kaluzny, J., Wysocka, A., and Thompson, I. 1999, astro-ph/9908041.
- Udalski, A., Szymański, M., Kaluzny, J., Kubiak, M., and Mateo, M. 1993, *Acta Astron.*, **43**, 69.
- Udalski, A., Olech, A., Szymański, M., Kaluzny, J., Kubiak, M., Mateo, M. and Krzemiński, W. 1995, *Acta Astron.*, **45**, 433.
- Udalski, A., Kubiak, M., and Szymański, M. 1997, *Acta Astron.*, **47**, 319.
- Udalski, A. 1998a, *Acta Astron.*, **48**, 113.
- Udalski, A. 1998b, *Acta Astron.*, **48**, 383.
- Udalski, A., Szymański, M., Kubiak, M., Pietrzyński, G., Woźniak, P., and Żebruń, K. 1998a, *Acta Astron.*, **48**, 1.
- Udalski, A., Szymański, M., Kubiak, M., Pietrzyński, G., Woźniak, P., and Żebruń, K. 1998b, *Acta Astron.*, **48**, 147.